Fusion Dynamics for Hot Fusion Reactions revealed in Quasielastic Fusion Barrier Distributions

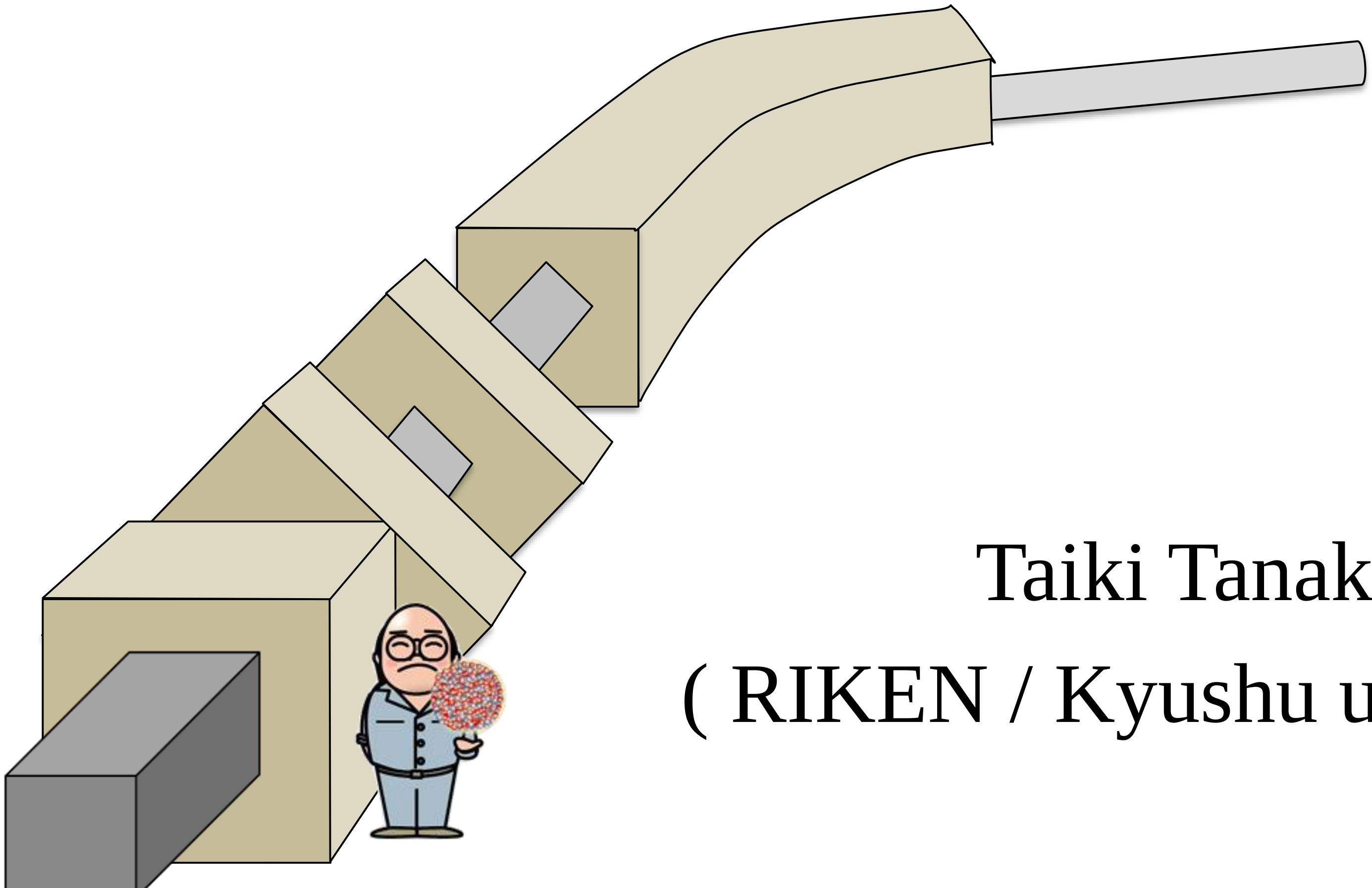

Taiki Tanaka

(RIKEN / Kyushu university)

Collaborators

Taiki Tanaka[1,2] , Kosuke Morita[1,2], Kouji Morimoto[1], Daiya Kaji[1],
Hiromitsu Haba[1], Rose Ann Boll[3] , Nathan T. Brewer[3,4],
Shelley Van Cleve[3], David Jarvis Dean[3], Satoshi Ishizawa[1,5],
Yuta Ito[1], Yukiko Komori[1], Katsuhisa Nishio[6], Toshitaka Niwase[1,2],
B. C. Rasco[3,4], James B. Roberto[3], Krzysztof P. Rykaczewski[7] ,
Hideyuki Sakai[1], Daniel W. Stracener[3], and Kouichi Hagino[8]

[1]RIKEN, [2]Kyushu university, [3]ORNL, [4]JINPA, [5]Yamagata university,
[6]Japan Atomic Energy Agency, [7]ORNL Physics Division,
[8]Tohoku university

Introduction

$^{48}Ca+^{248}Cm \rightarrow {}^{296}Lv^*$

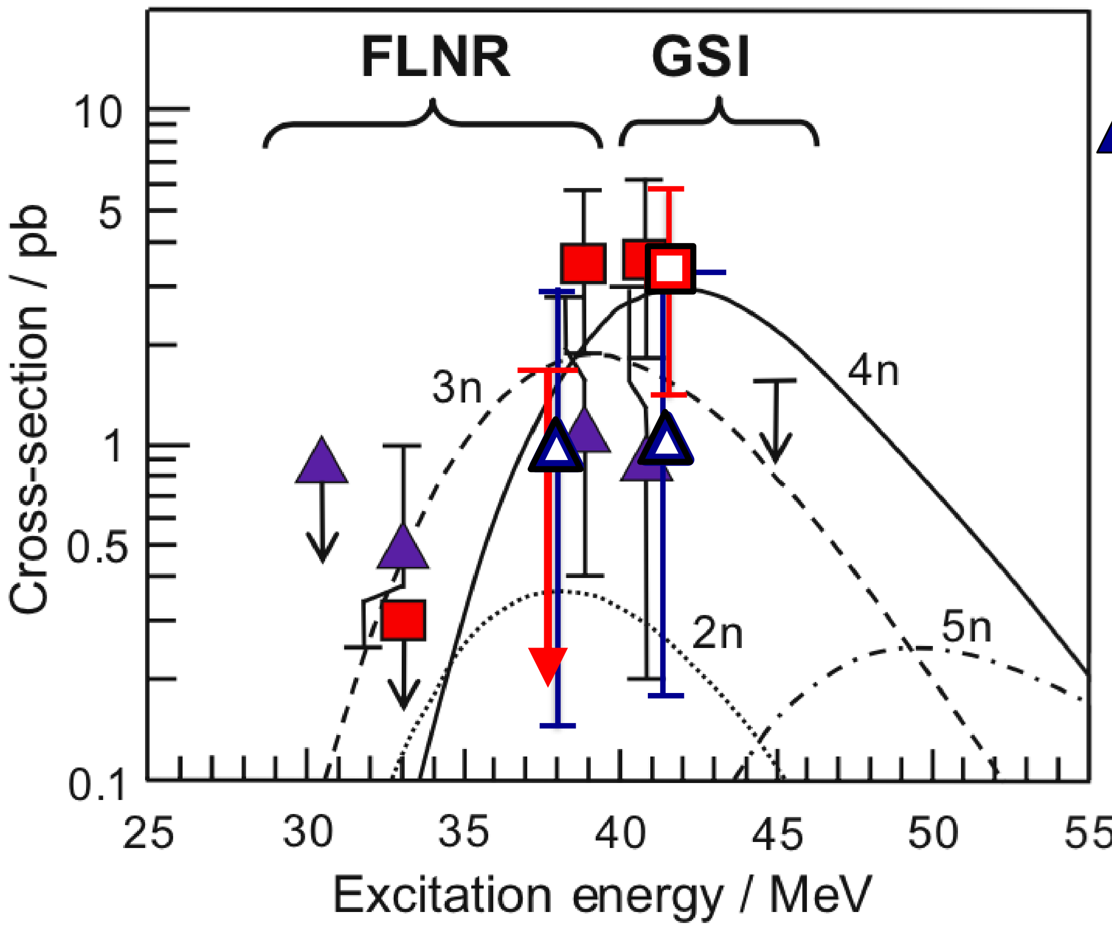

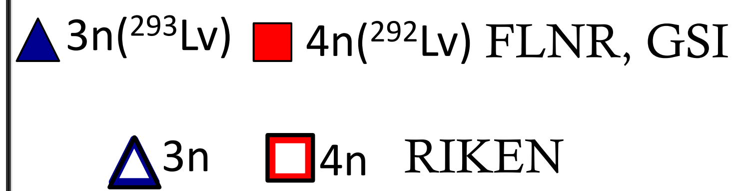

Yu. Ts. Oganessian *et al.*, Phys. Rev. C **70** 064609 (2004).

S. Hofmann *et al.*, Eur. Phys. J. A**48**, 62 (2012).

D. Kaji *et al.*, J. Phys. Soc. Jpn. **86**, 034201 (2017).

Calculated cross section from V. I. Zagrebaev, Nucl. Phys. A **734**, 164 (2004).

σ_{ER} strongly depends on the incident energy.

Fusion process of heavy reaction system

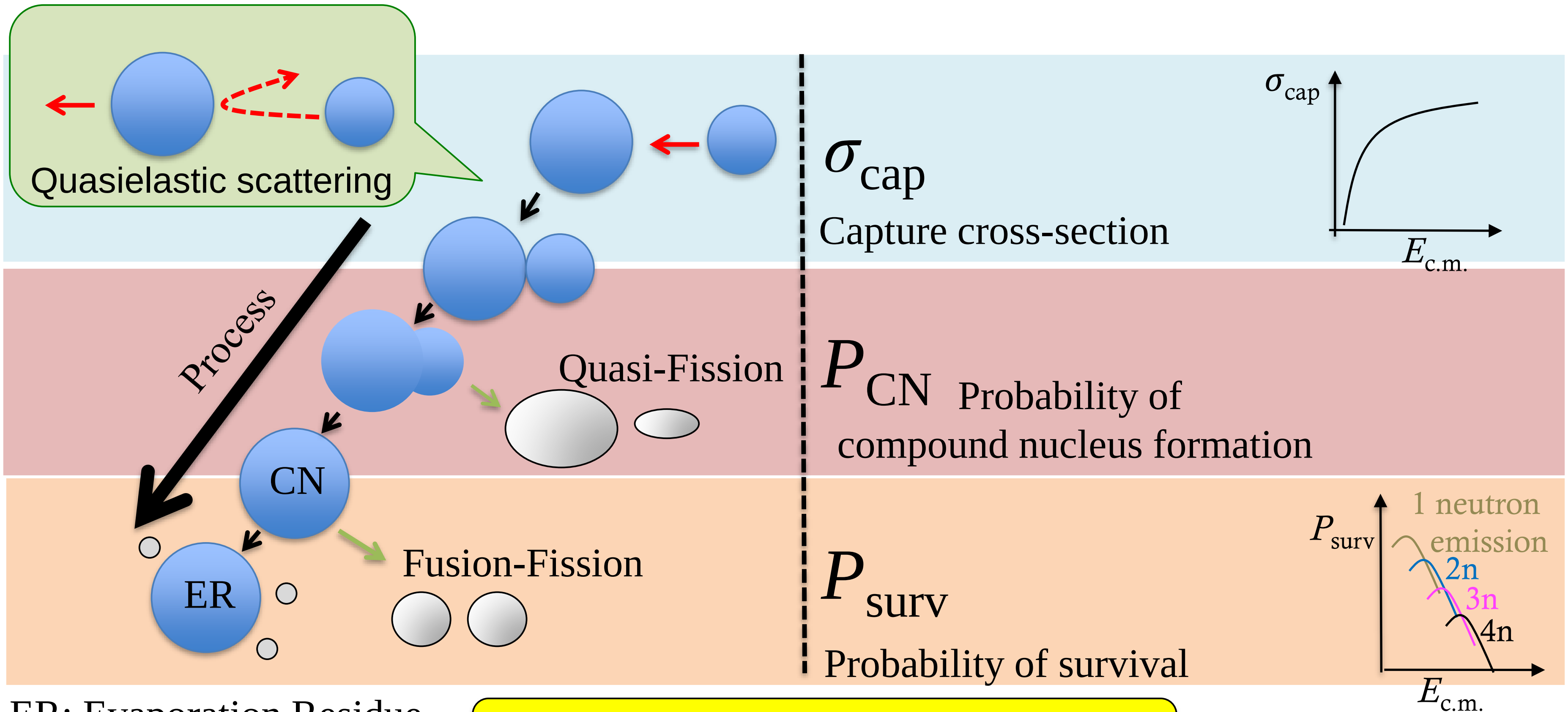

ER: Evaporation Residue
CN: Compound Nucleus

$$\sigma_{ER} = \sigma_{cap} \cdot P_{CN} \cdot P_{surv}$$

Synthesis S.H.N by using fusion reaction → Incident energy : near the coulomb barrier

Quasielastic scattering = Information of the fusion barrier distribution

What is the Coulomb barrier?

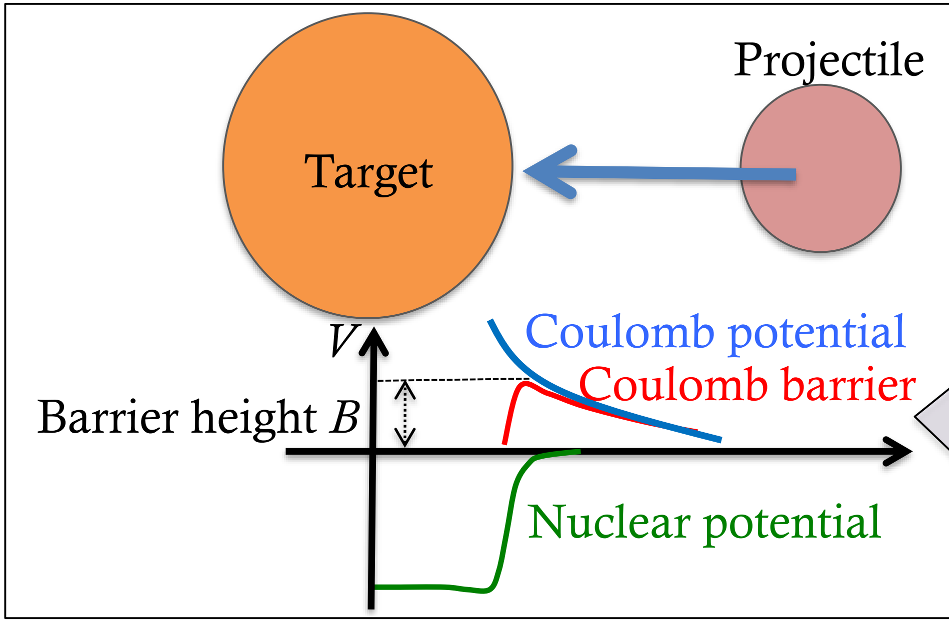

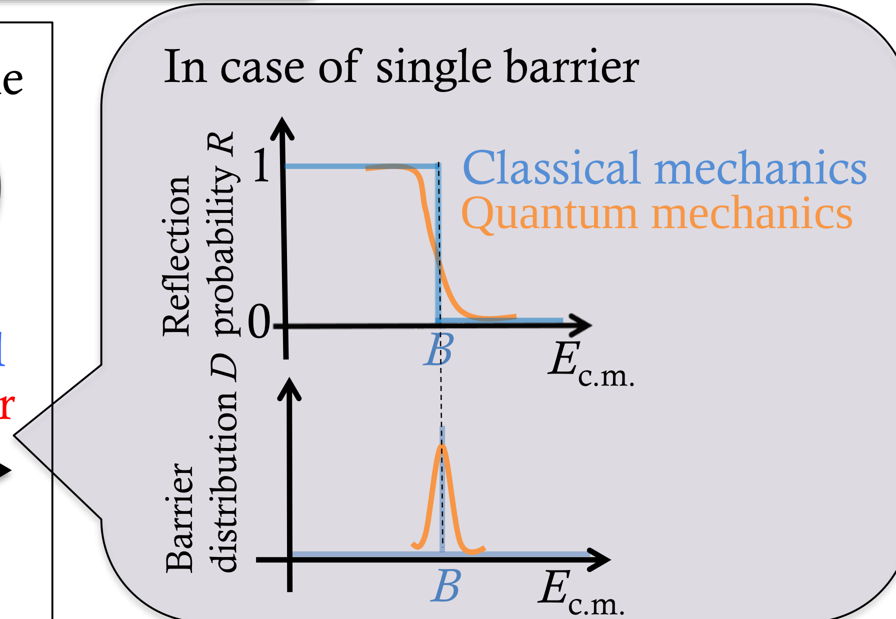

In case of deformed target

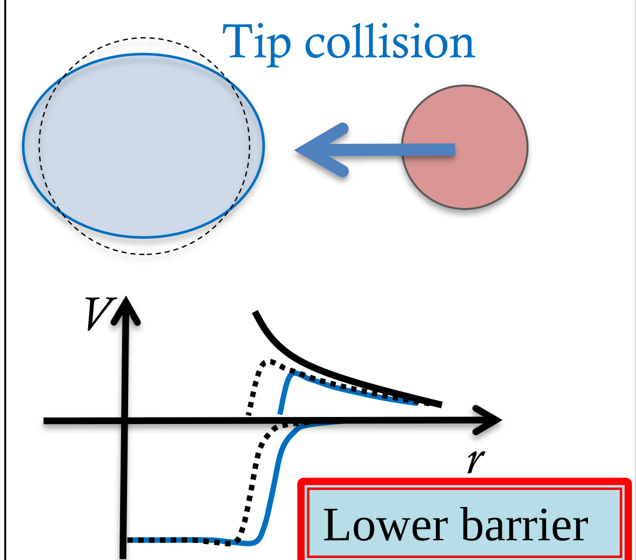

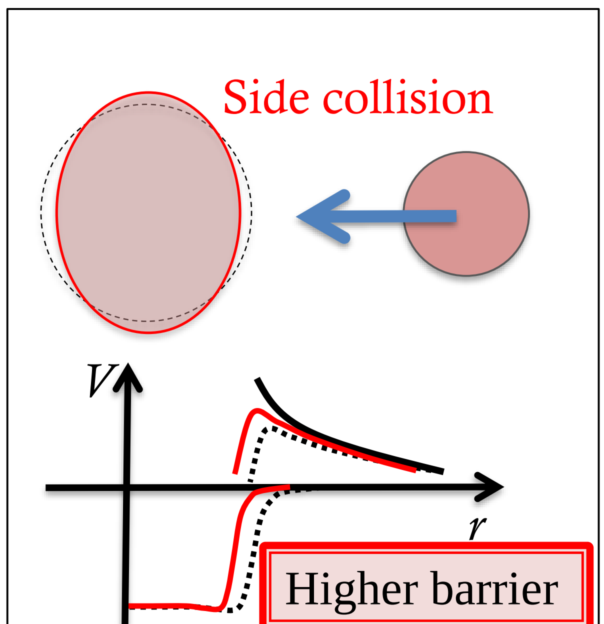

- Sum of the coulomb barriers for different angles
- Vibrational excitations

→ Make Coulomb barrier distribution

Measurements of barrier distributions

How to measure the barrier heights?

- From fusion cross-section
- From quasielastic scattering at large scattering angles — This work

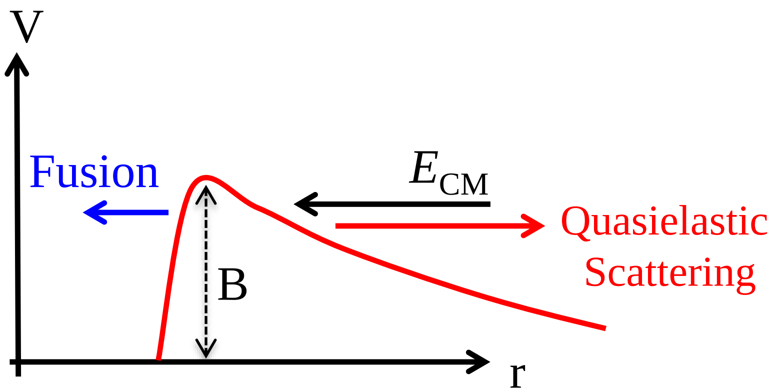

Quasielastic scattering = Except fusion reaction (Elastic scattering, Inelastic scattering…)

→ Detection of nucleus which recoiled by coulomb barrier

Reflection probability

$$R = \frac{\left(\frac{d\sigma}{d\Omega}\right)_{QE}}{\left(\frac{d\sigma}{d\Omega}\right)_{R}}$$

$\frac{\text{Quasielastic(QE) scattering cross-section}}{\text{Rutherford cross-section}}$

Barrier distribution

$$D_{QE}(E) = -\frac{d}{dE}\left(\frac{\sigma_{QE}(E,p)}{\sigma_{R}(E,p)}\right)$$

H. Timmers *et al.*, Nucl. Phys. A **584**, 190 (1995).
K. Hagino *et al.*, Phys. Rev. C **69**, 054610 (2004).

Previous research

Detection of the projectile nucleus which reflected to $\theta_{\mathrm{lab}} = 172^{\circ}$

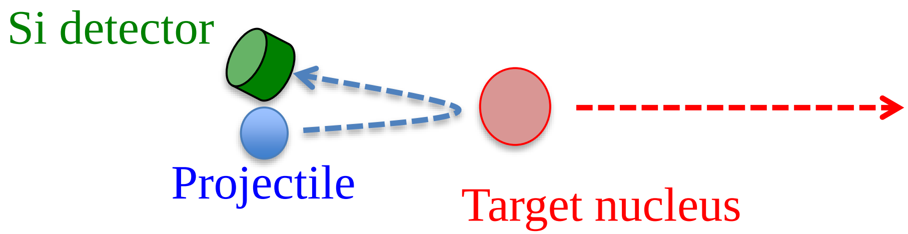

S. Mitsuoka *et al.*,
Phys. Rev. Lett. **99**, 182701 (2007).

This work

Detection of the target nucleus which recoiled to $\theta_{\mathrm{lab}} = 0^{\circ}$

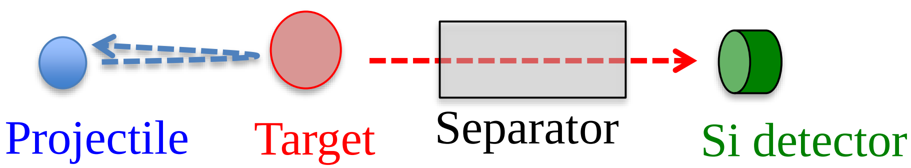

T. Tanaka *et al.*,
J. Phys. Soc. Jpn. **87**, 014201 (2018).

Corresponding to measurement of the projectile nucleus at $\theta_{\mathrm{lab}} = 180^{\circ}$

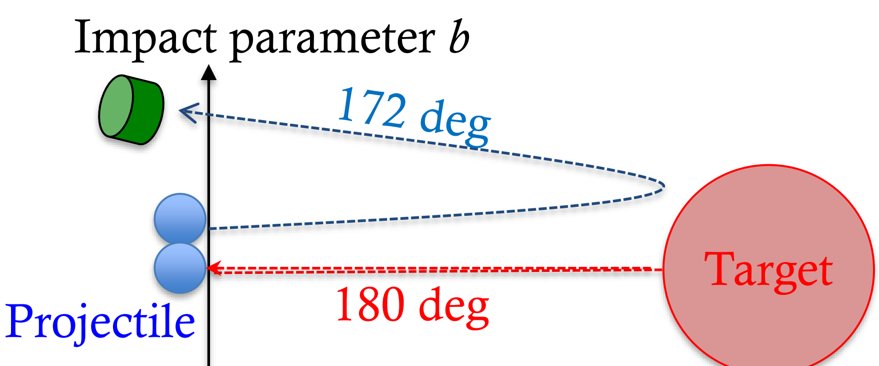

Impact parameter $b \propto$ Angular momentum L

Deriving the fusion barrier B_{fu} $(L \sim 0)$ directly

Measurements of barrier distributions with GARIS

T. Tanaka *et al.*, J. Phys. Soc. Jpn. **87**, 014201 (2018).

GARIS

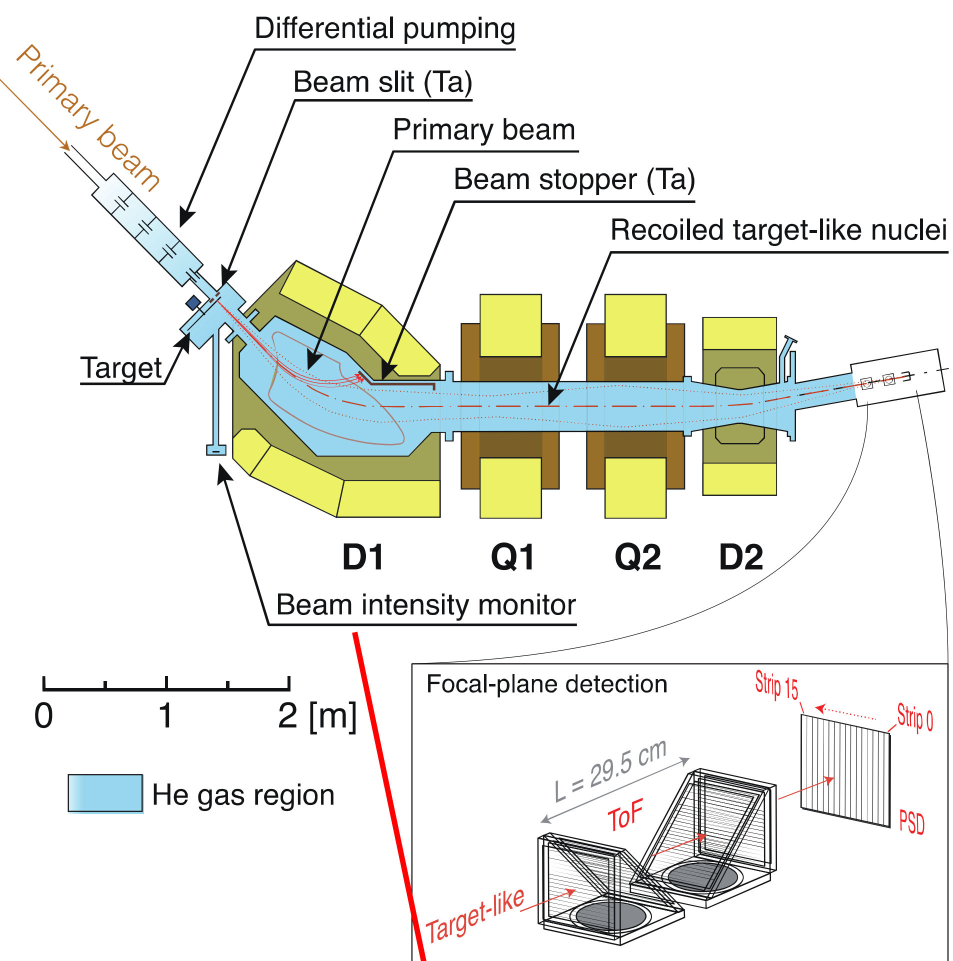

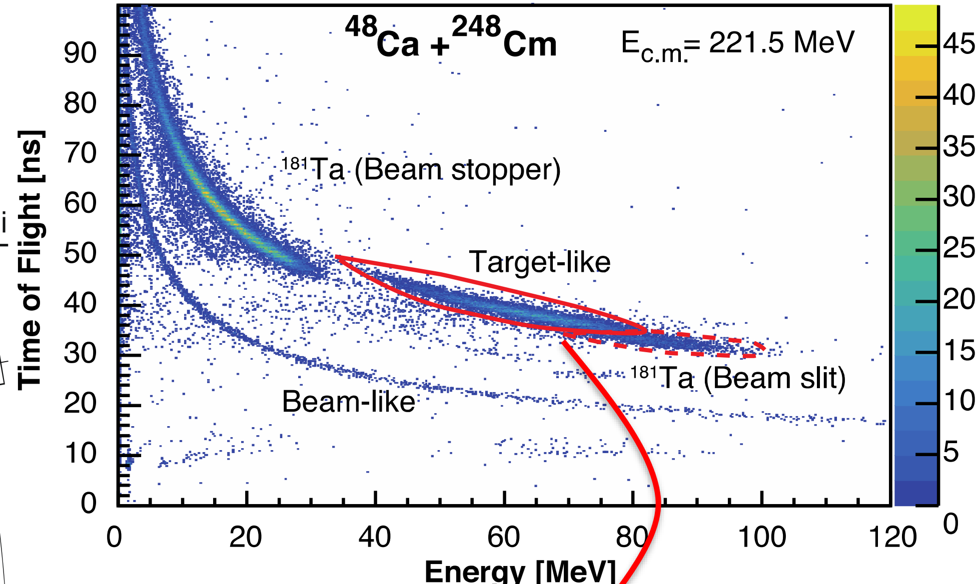

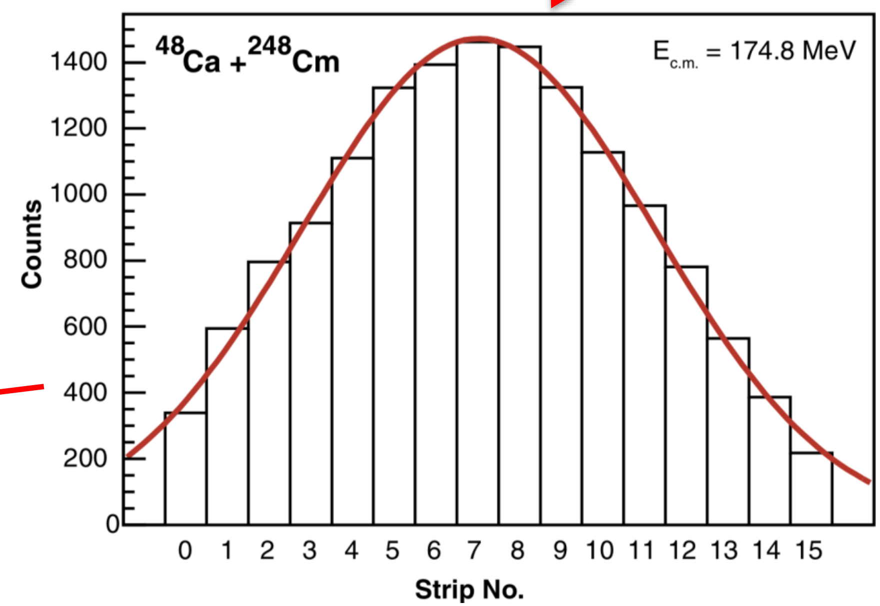

$$D_{QE}(E) = -\frac{d}{dE}\left(\frac{\sigma_{QE}(E,p)}{\sigma_{R}(E,p)}\right)$$

Experimental results

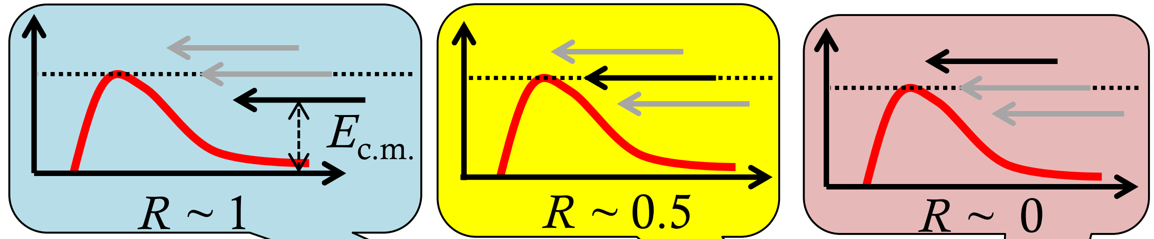

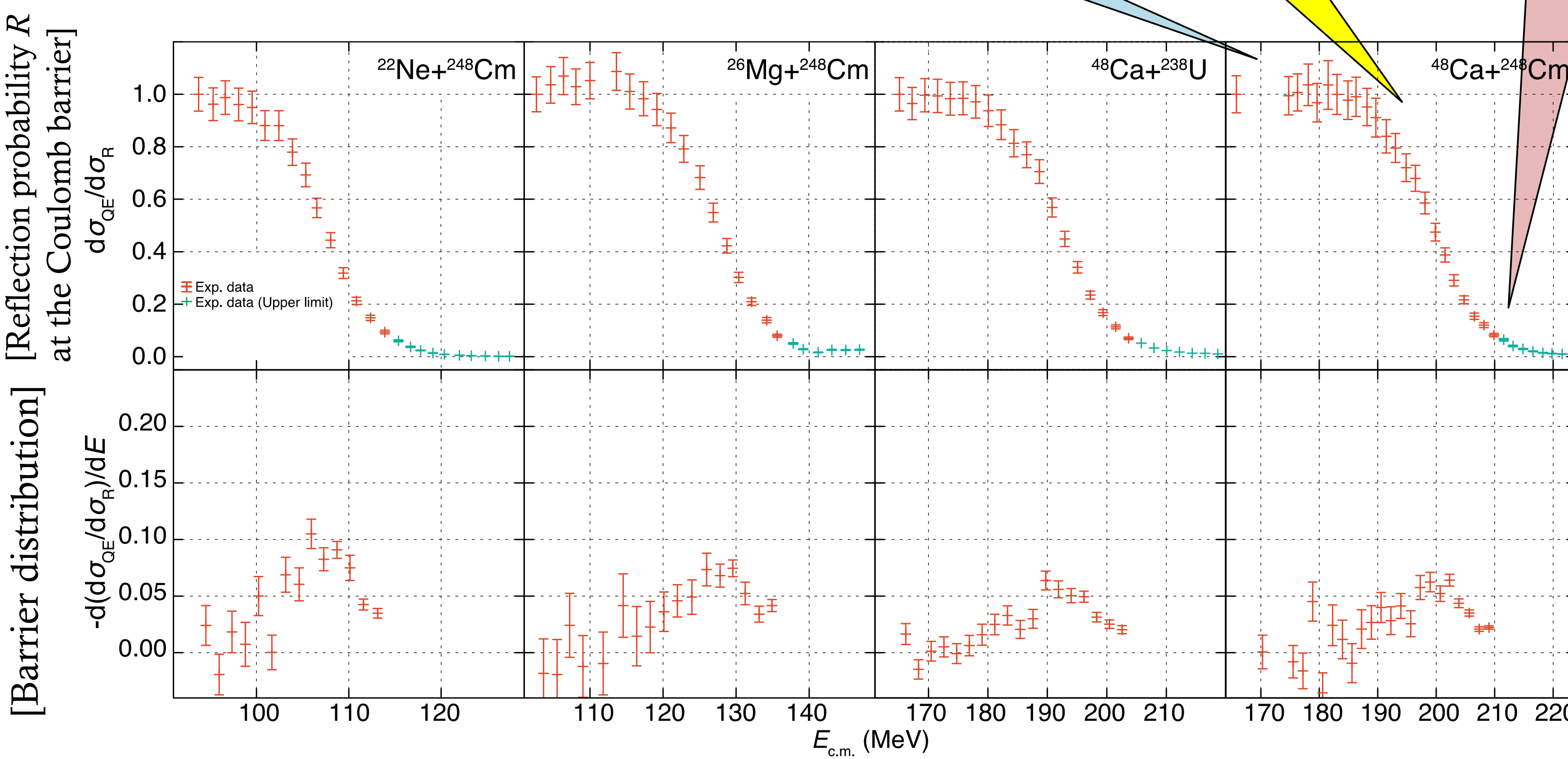

Reflection probability decreases with increasing the $E_{c.m.}$
(Beyond the Coulomb barrier)

Deep-inelastic scattering events

Previous research

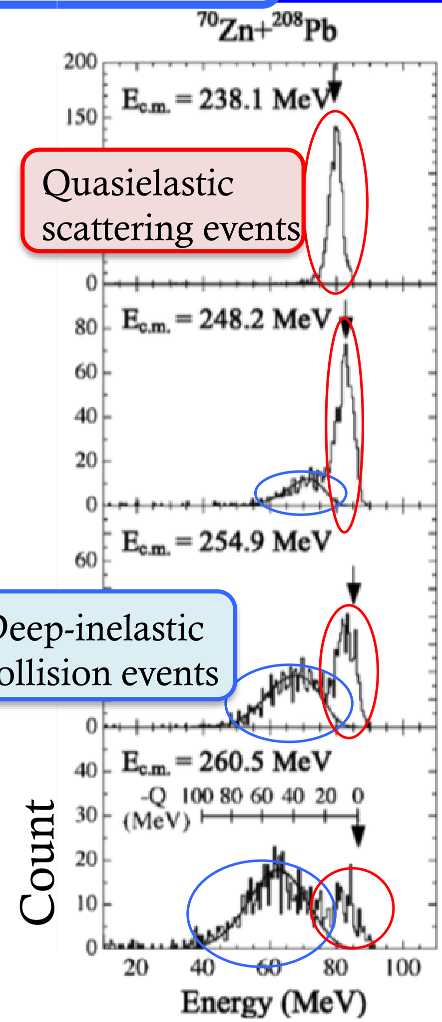

S. Mitsuoka *et al.*, PRL99('07) 182701

This work

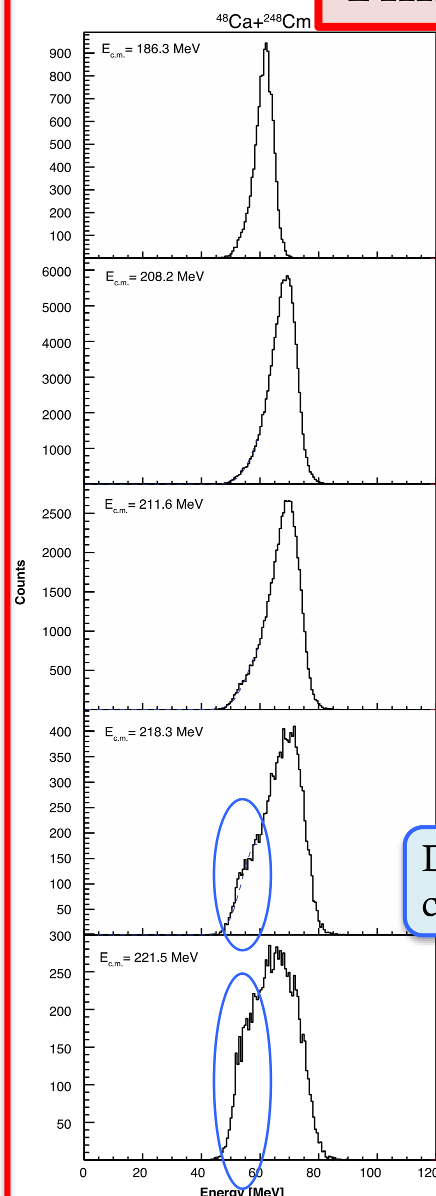

Deep-inelastic collision events

Deep-inelastic scattering events

$^{40}Ar+^{248}Cm$, $E_{c.m.} = 193.8$ MeV

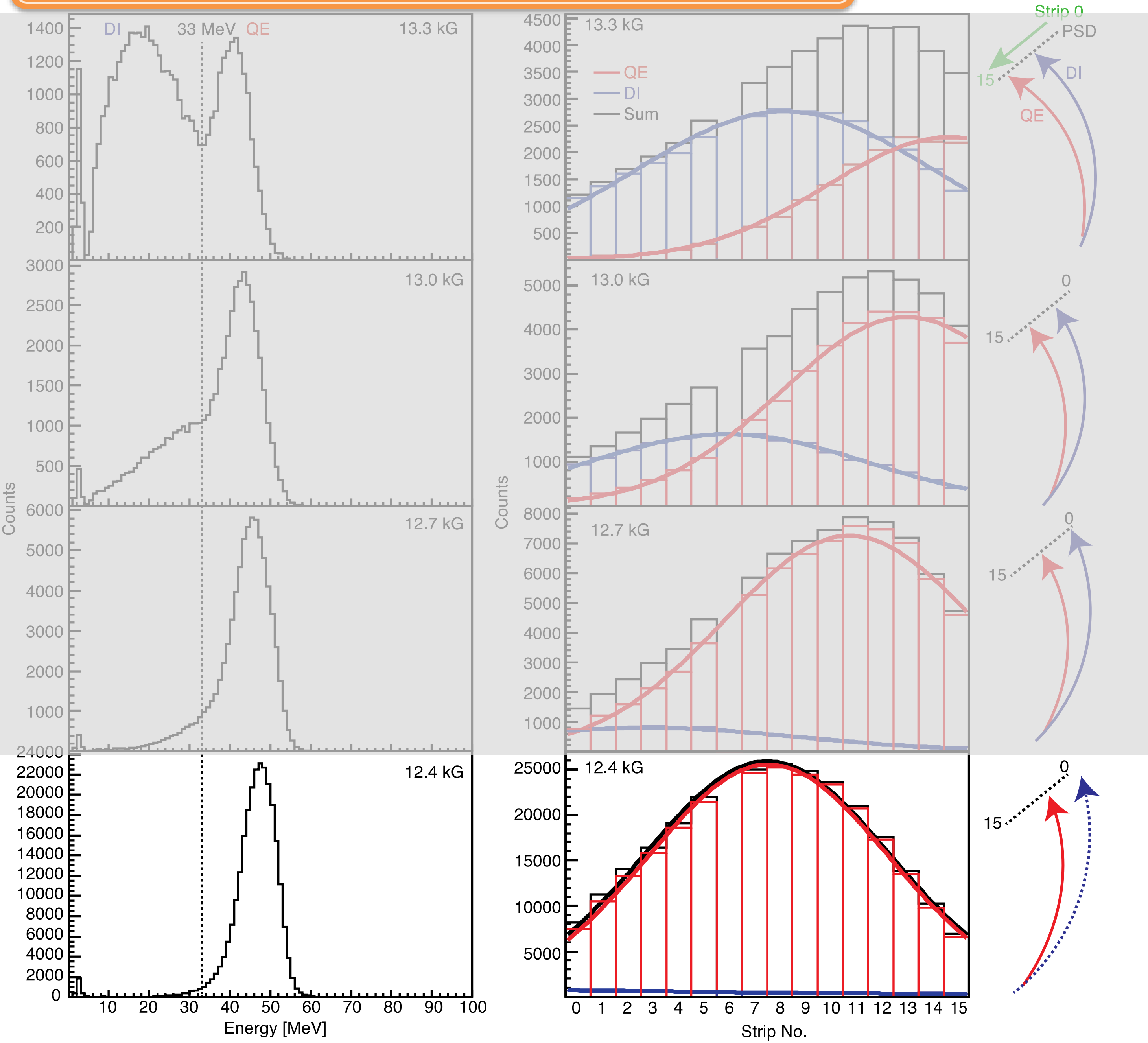

Quasielastic scattering event dominant region

Deep-inelastic scattering events

$^{40}Ar+^{248}Cm$, $E_{c.m.}$ = 193.8 MeV

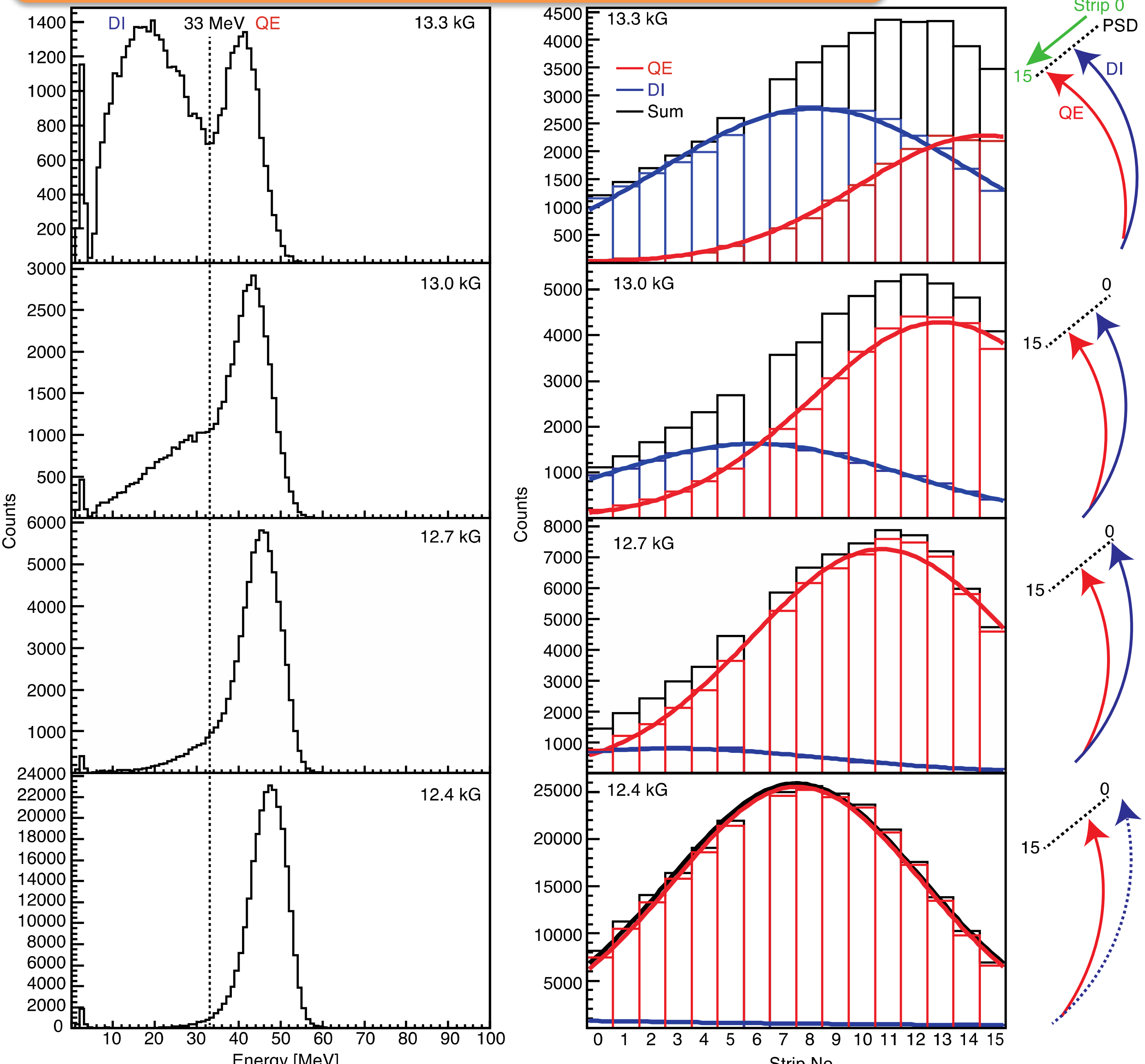

Deep-inelastic scattering event dominant region

Quasielastic scattering event dominant region

Deep-inelastic scattering events

$^{40}Ar+^{248}Cm$, $E_{c.m.}$ = 193.8 MeV

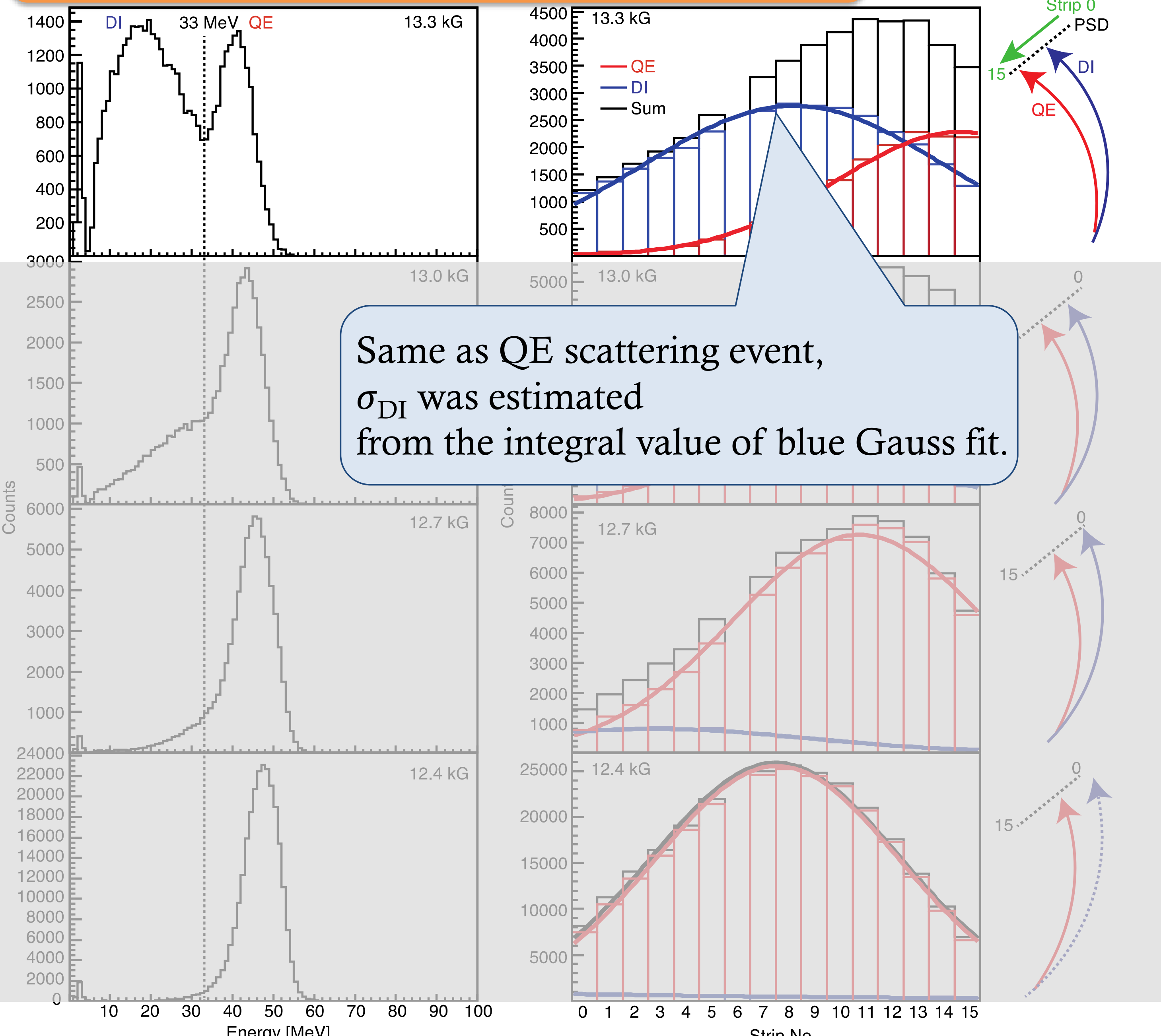

Same as QE scattering event,
σ_{DI} was estimated
from the integral value of blue Gauss fit.

Deep-inelastic scattering event dominant region

Quasielastic scattering event dominant region

Upper limit for deep-inelastic scattering events

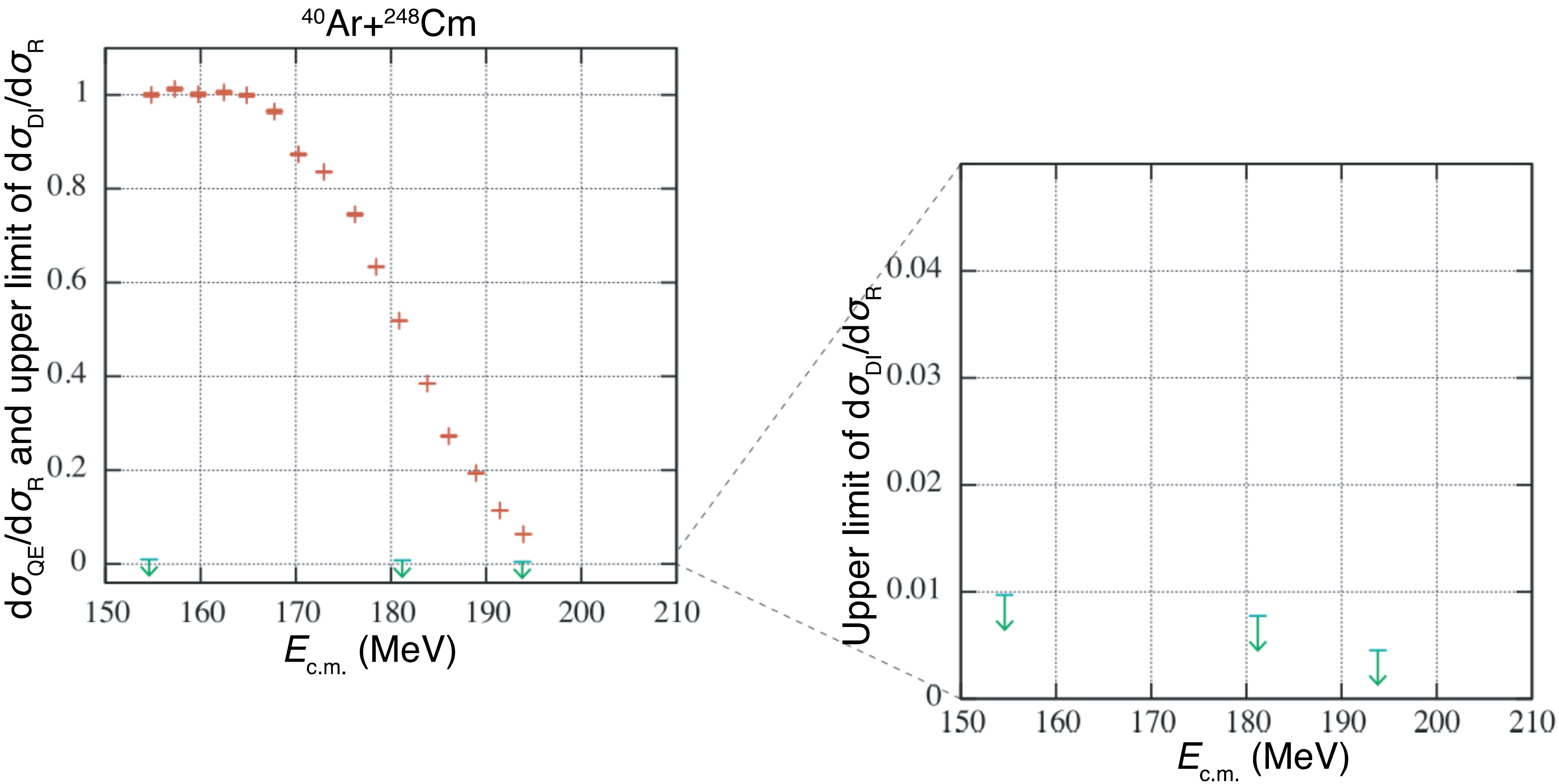

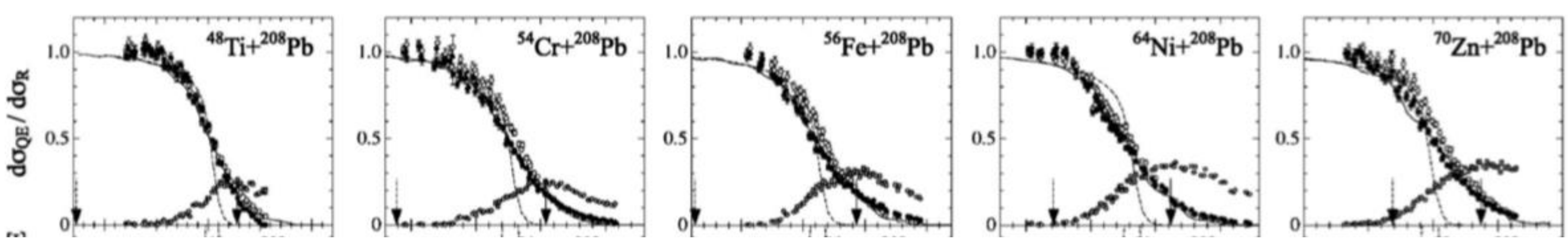

S. Mitsuoka *et al.*, Phys. Rev. Lett. **99**, 182701 (2007).

Comparison with coupled-channels calculation CCFULL*

Single channel (without any coupling)

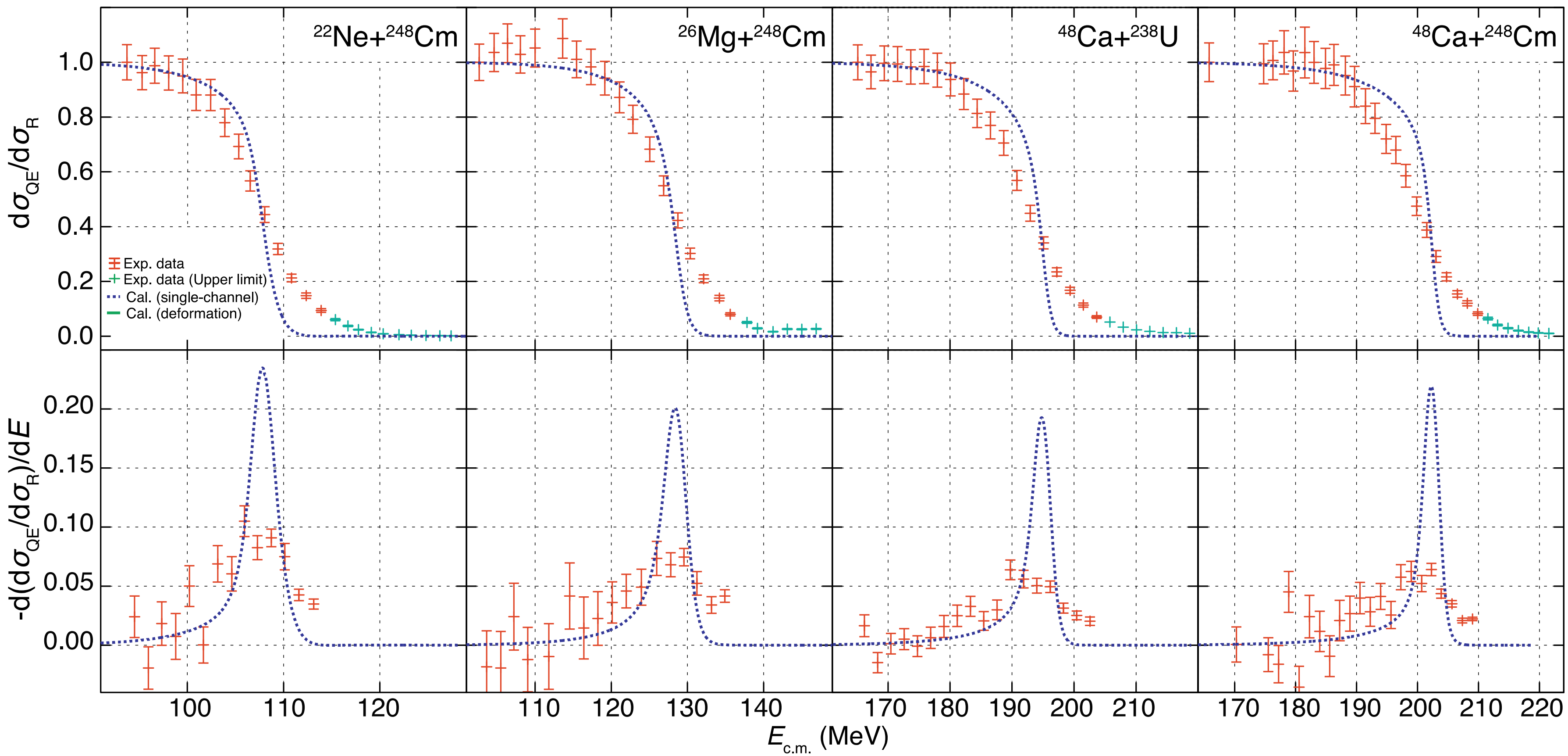

V_0 = 52.0 MeV, r_0 = 1.18fm, a_0 = 0.69 fm
V_w = 50.0 MeV, r_w = 1.08fm, a_w = 0.25 fm

V_0 = 56.0 MeV, r_0 = 1.18fm, a_0 = 0.69 fm
V_w = 50.0 MeV, r_w = 1.08fm, a_w = 0.40 fm

V_0 = 70.0 MeV, r_0 = 1.18fm, a_0 = 0.69 fm
V_w = 50.0 MeV, r_w = 1.08fm, a_w = 0.40 fm

V_0 = 80.0 MeV, r_0 = 1.18fm, a_0 = 0.69 fm
V_w = 50.0 MeV, r_w = 1.00fm, a_w = 0.40 fm

* K. Hagino *et al.*, Comput. Phys. Comm. **123** (1999) 143

Comparison with coupled-channels calculation CCFULL

Single channel (without any coupling)
Deformation

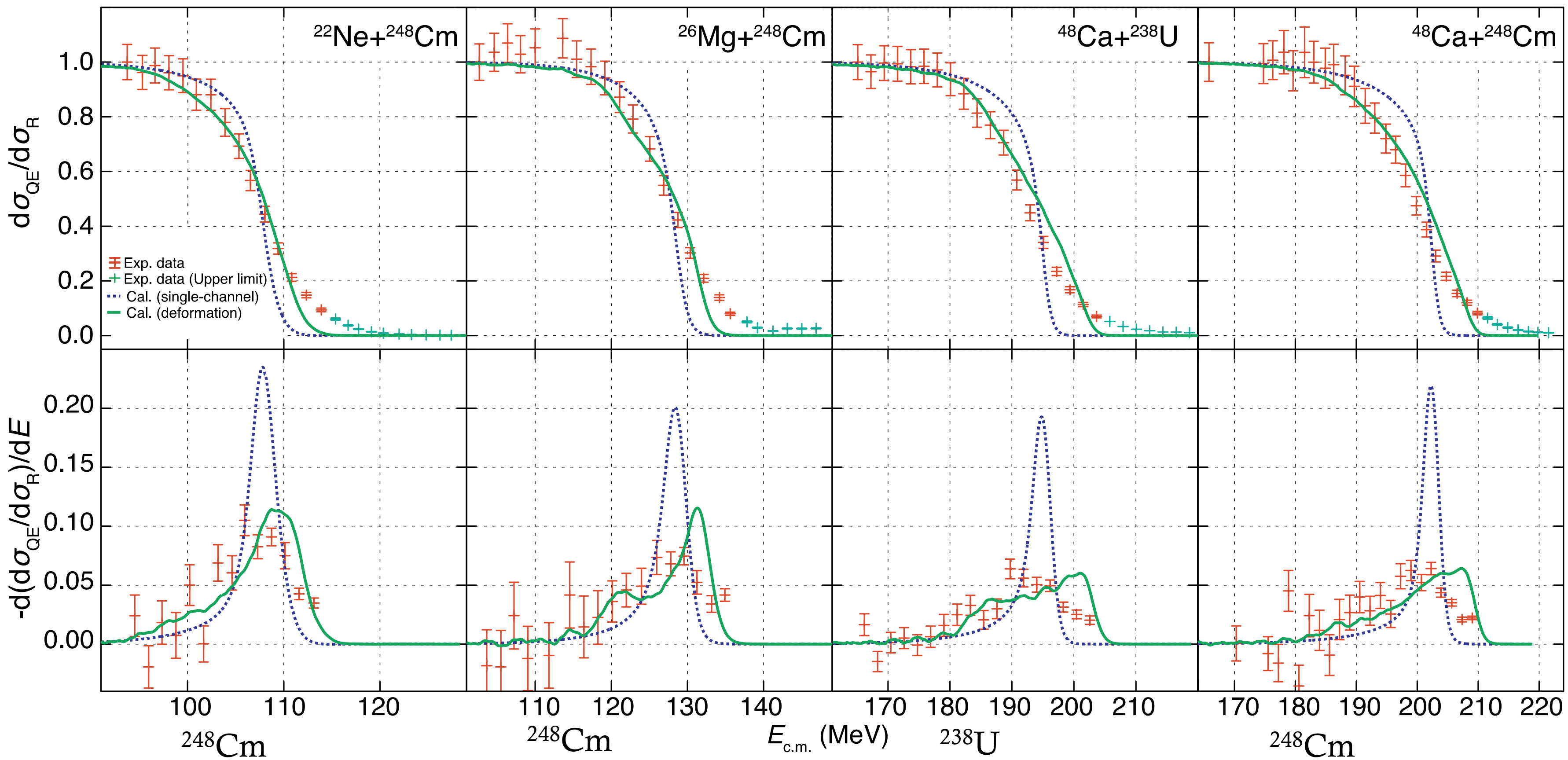

^{248}Cm	^{248}Cm	^{238}U	^{248}Cm
β_2 = 0.2972 [1]	β_2 = 0.2972 [1]	β_2 = 0.2860 [1]	β_2 = 0.286 [3]
β_4=0.039 [2]	β_4=0.039 [2]	β_4=-0.02	β_4=0.03
β_6 = 0.030	β_6 = -0.030	β_6 = 0.00	β_6 = 0.020

[1] S. Raman *et al.*, At. Data Nucl. Data Tables 78, 1 (2001).
[2] P. Moller *et al.*, At. Data Nucl. Data Tables 109-110, 1-204 (2016).
[3] S. Raman *et al.*, At. Data Nucl. Data Tables 36, 1 (1987).

Barrier distributions are strongly affected by the deformation.

Comparison with coupled-channels calculation CCFULL

Single channel (without any coupling)
Deformation
Full (Deformation+excited)

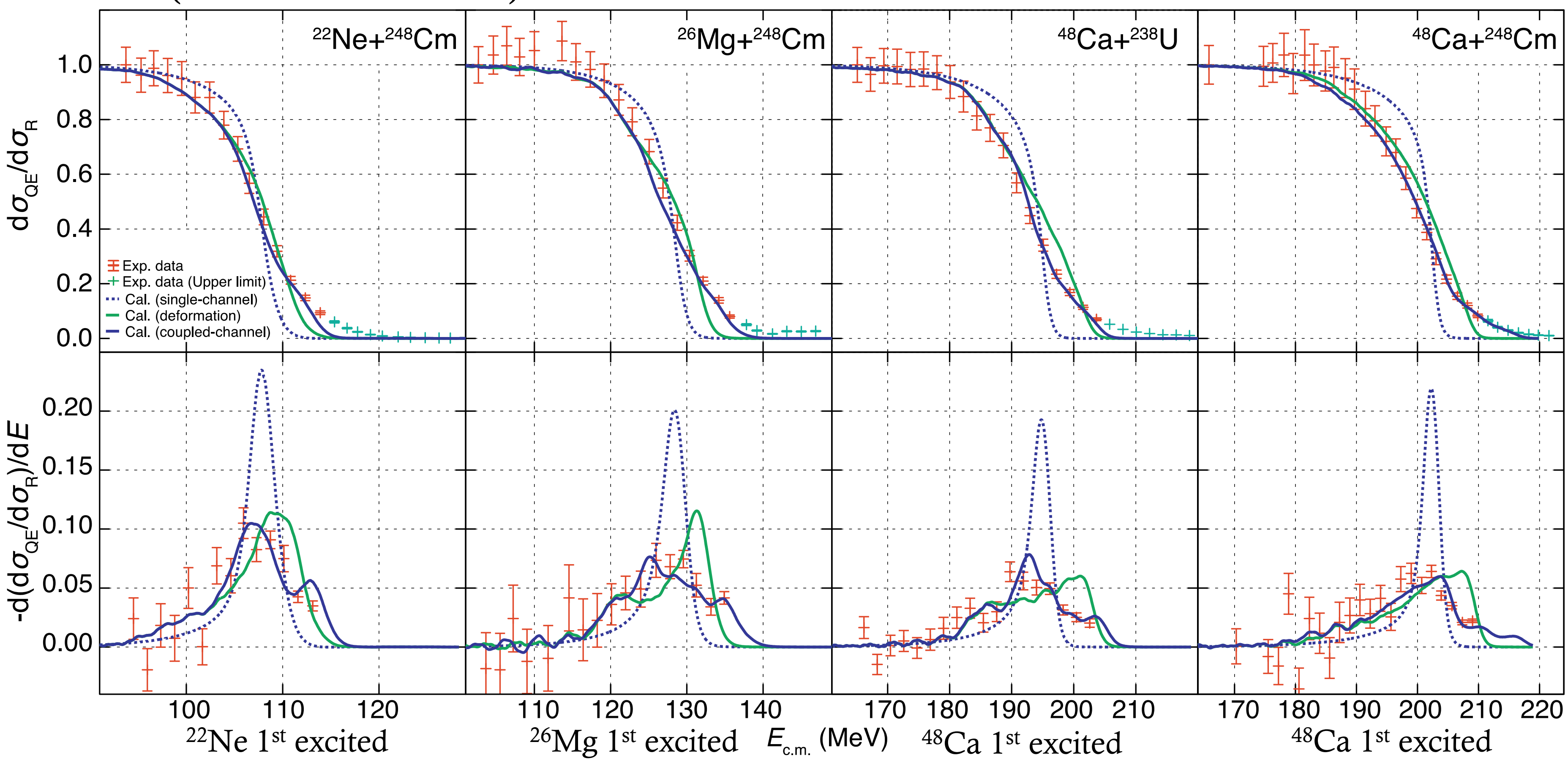

^{22}Ne 1st excited (1.27 MeV, 2+) + 1n transfer

^{26}Mg 1st excited (1.81 MeV, 2+) + 1n transfer

^{48}Ca 1st excited (4.507 MeV, 3-) + 1n transfer

^{48}Ca 1st excited (4.507 MeV, 3-) + 1n transfer

Barrier distributions are strongly affected by the deformation.

+ Improvement by excited states and 1n transfer

Comparison with barrier distributions and σ_{ER}

Hot fusion reactions
($^{22}Ne+^{248}Cm$, $^{26}Mg+^{248}Cm$, $^{48}Ca+^{238}U$, $^{48}Ca+^{248}Cm$)

T. Tanaka *et al.*,
J. Phys. Soc. Jpn. **87**, 014201 (2018).

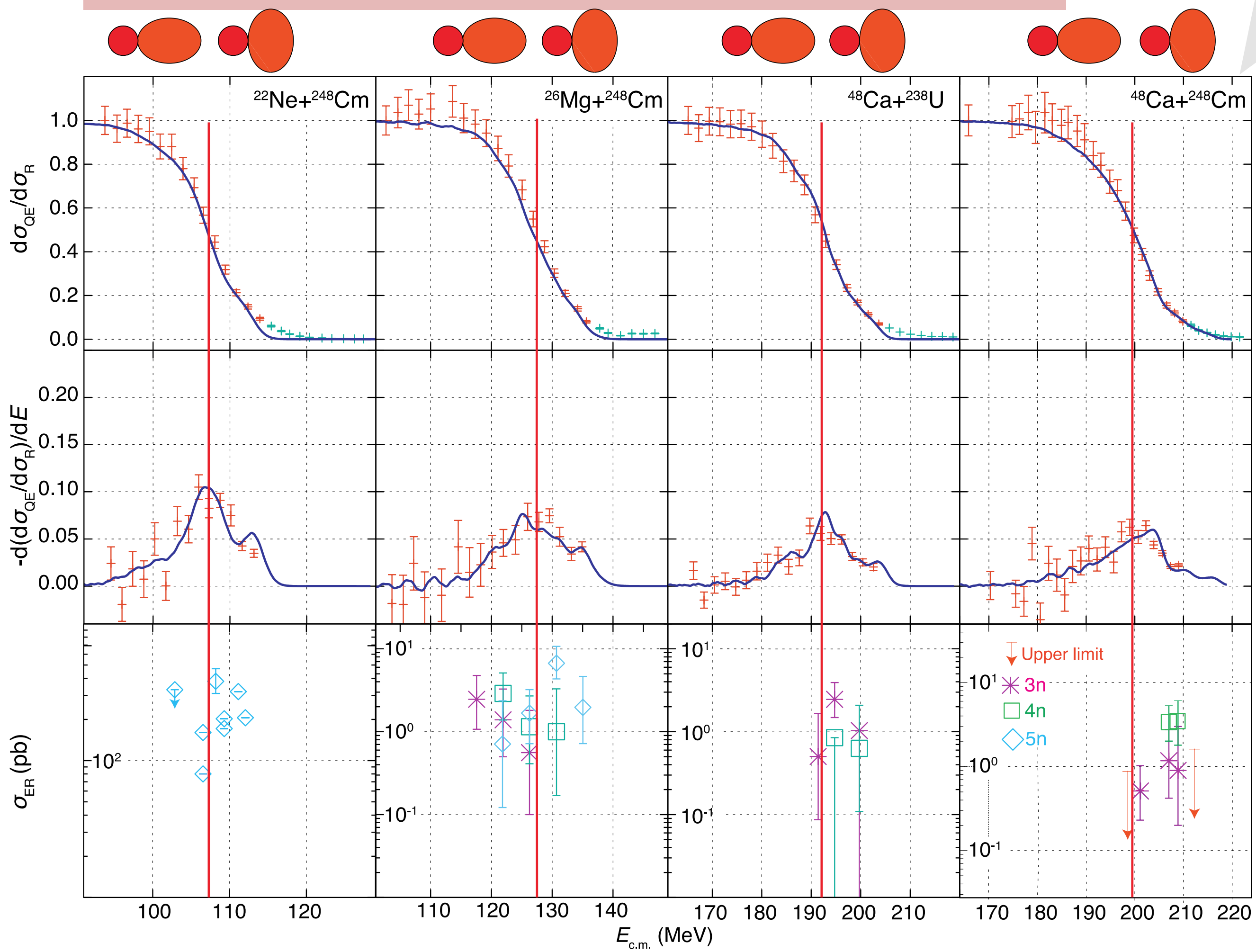

Z = 106 (Sg) Z = 108 (Hs) Z = 112 (Cn) Z = 116 (Lv)

Peaks of the σ_{ER} appear well above the average Coulomb barrier B_0 ($d\sigma_{QE}/ d\sigma_R = 0.5$)

Coulomb barrier heights for deformed target nucleus

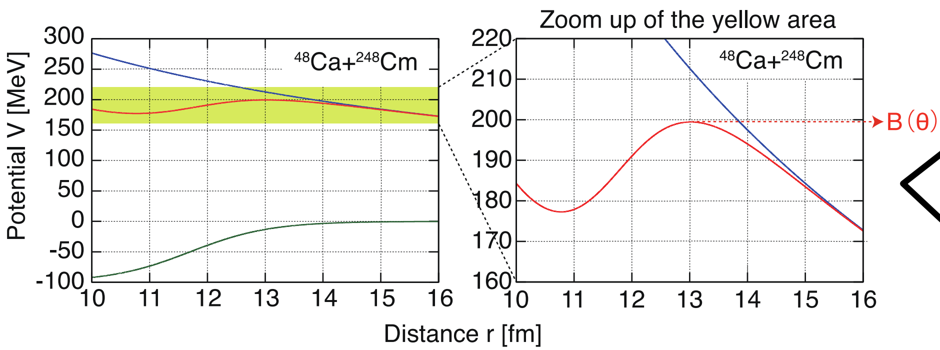

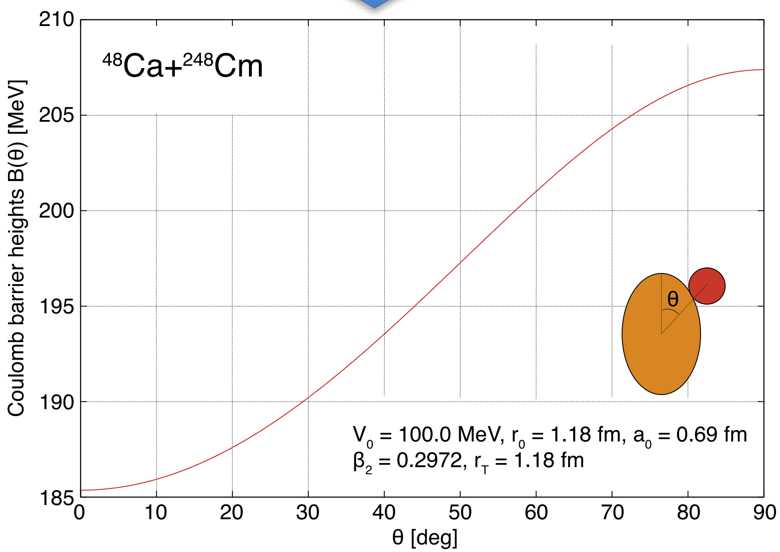

$$V_N(r,\theta) = -\frac{V_0}{1+\exp[\{r - R_0 - R_T \sum_\lambda \beta_{\lambda T} Y_{\lambda 0}(\theta)\}/a]}, \tag{16}$$

$$\begin{aligned} V_C(r,\theta) = {} & \frac{Z_P Z_T e^2}{r} \\ & + \frac{3 Z_P Z_T e^2}{5} \frac{R_T^2}{r^3} \left(\beta_{2T} + \frac{2}{7}\sqrt{\frac{5}{\pi}} \beta_{2T}^2 \right) Y_{20}(\theta) \\ & + \frac{3 Z_P Z_T e^2}{9} \frac{R_T^4}{r^5} \left(\beta_{4T} + \frac{9}{7\sqrt{\pi}} \beta_{2T}^2 \right) Y_{40}(\theta) \\ & + \frac{3 Z_P Z_T e^2}{13} \frac{R_T^6}{r^7} \beta_{6T} Y_{60}(\theta), \end{aligned} \tag{17}$$

K. Hagino, Phys. Rev. C **98**, 014607 (2018).

$$B_0 = \frac{\int_0^{\pi/2} B(\theta)\sin(\theta)\,d\theta}{\int_0^{\pi/2} \sin(\theta)\,d\theta}$$

Example; ^{48}Ca+^{248}Cm

B_0 = 199.5 MeV

Change the V_0 to reproduce the B_0

$B_{\text{side (= 90 deg)}}$ = 207.4 MeV

Coulomb barrier of the side collision B_{side}

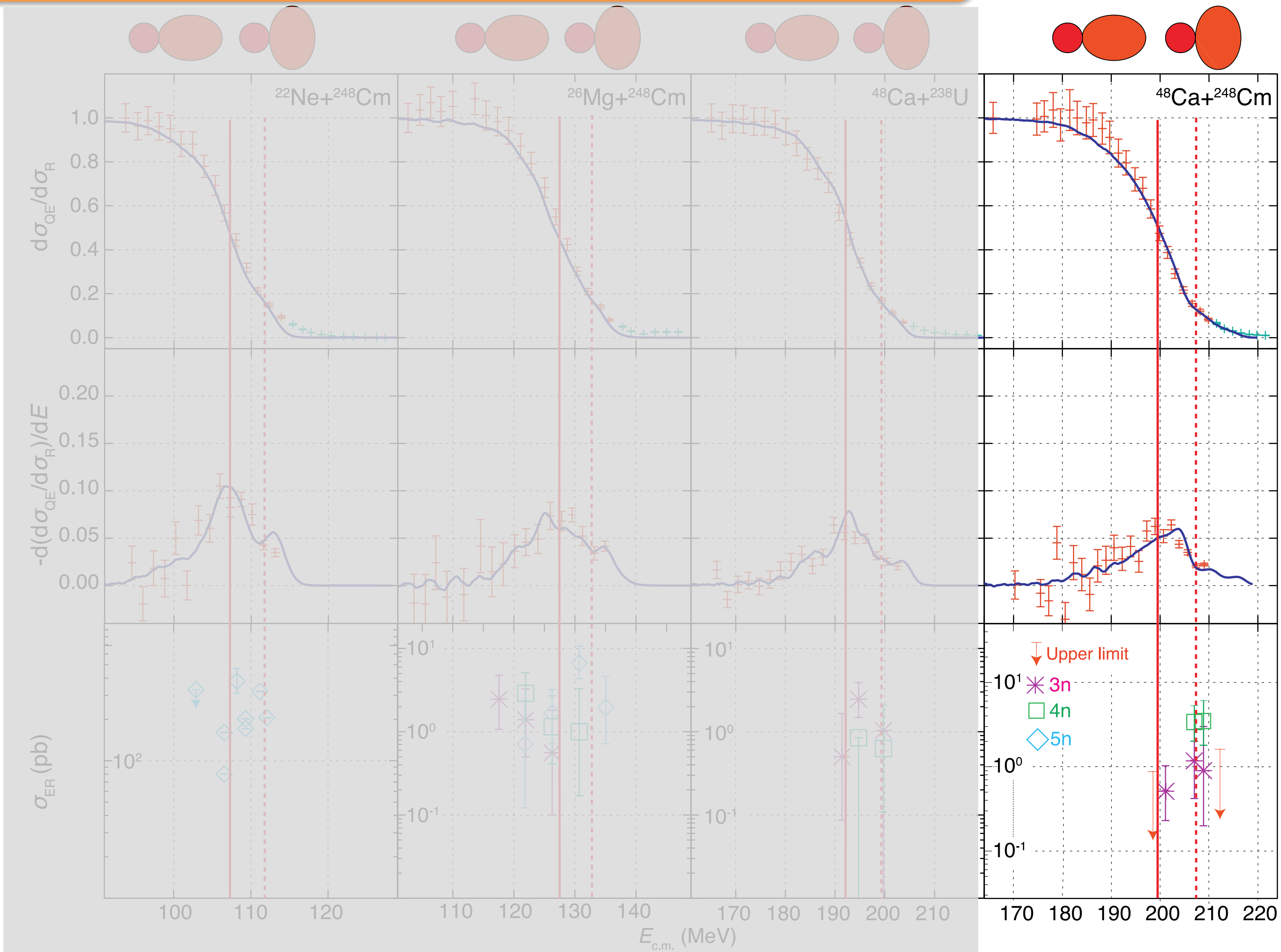

Coulomb barrier of the side collision B_{side}

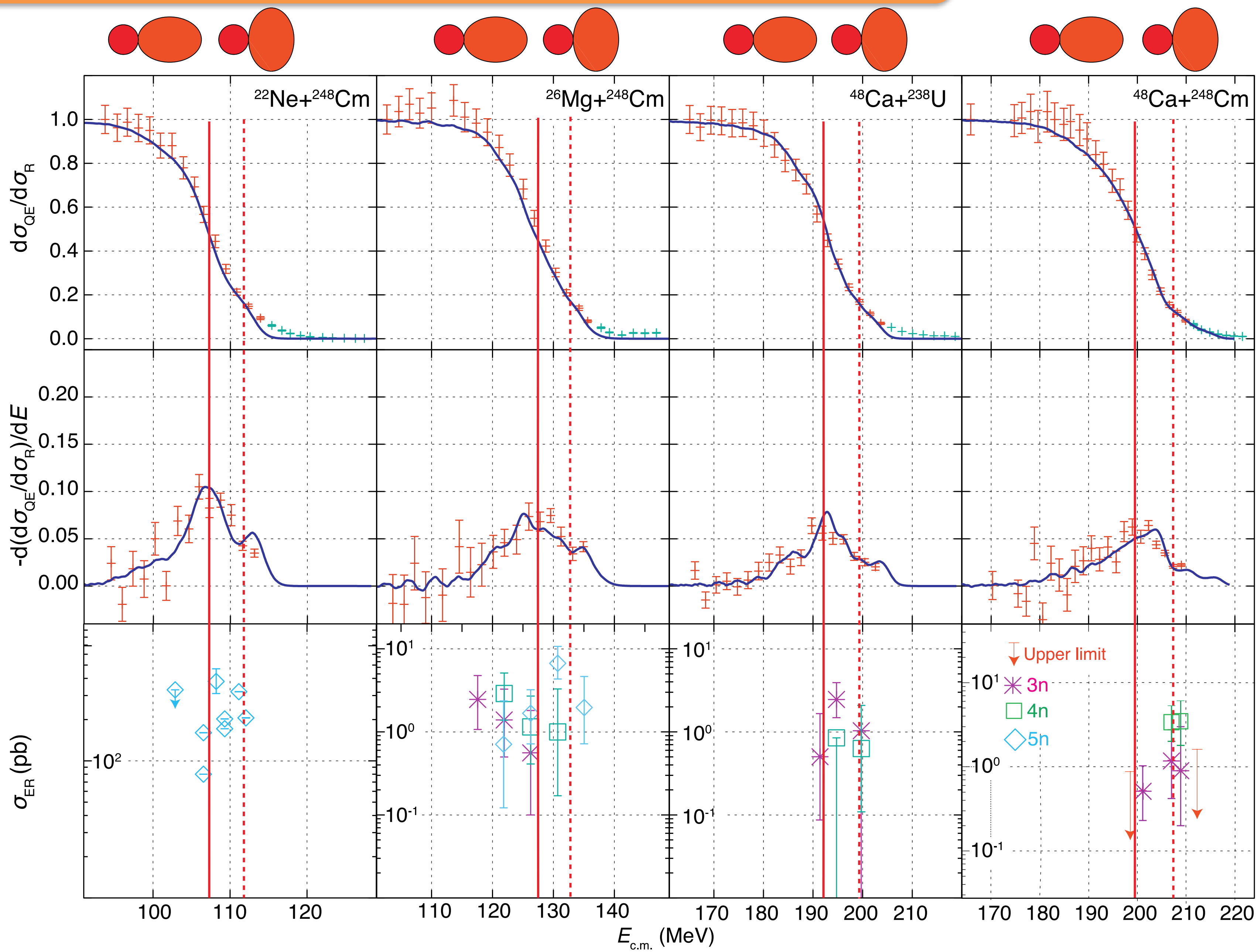

Coulomb barrier of the side collision B_{side}

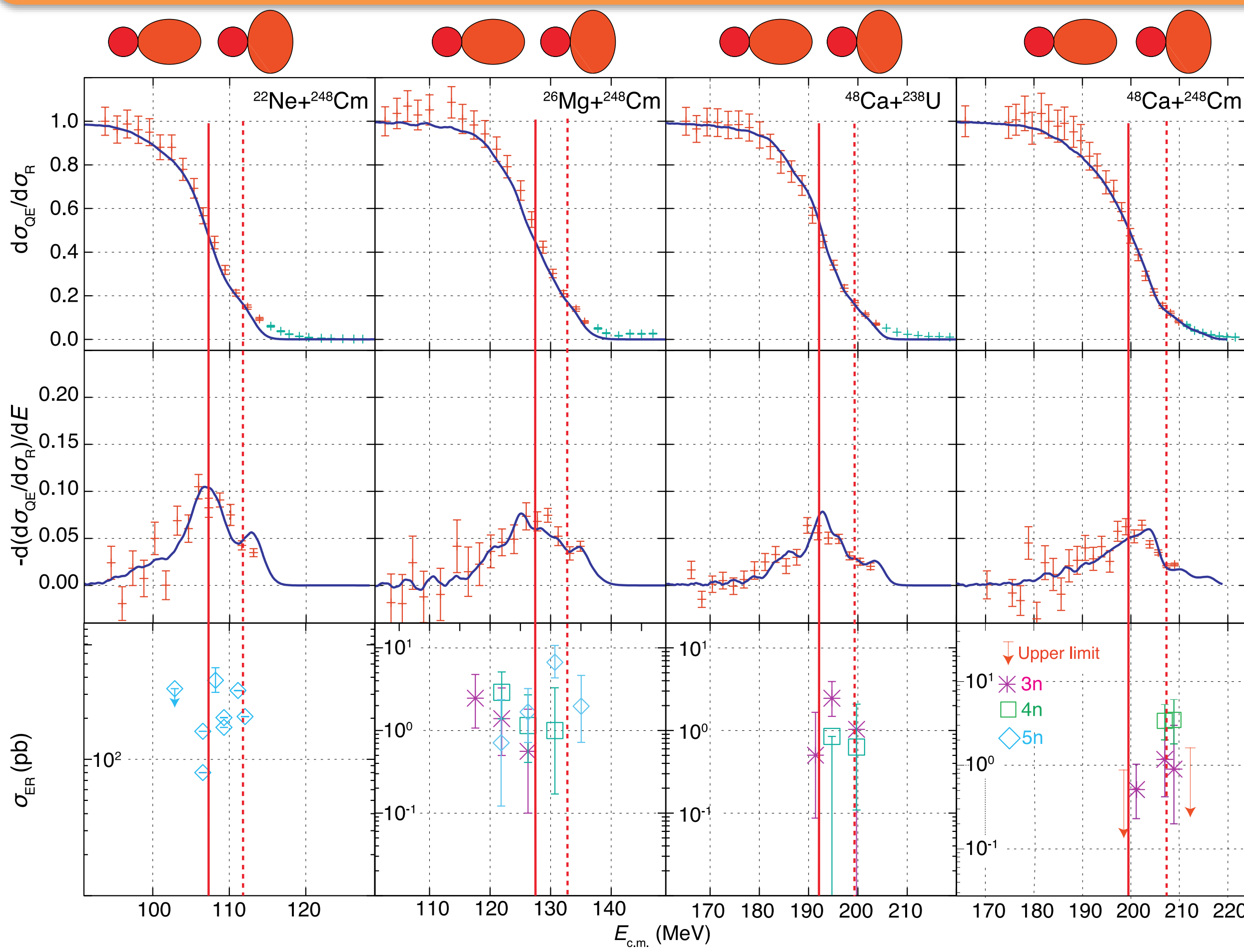

Peaks of σ_{ER} appear between B_0 and B_{side}

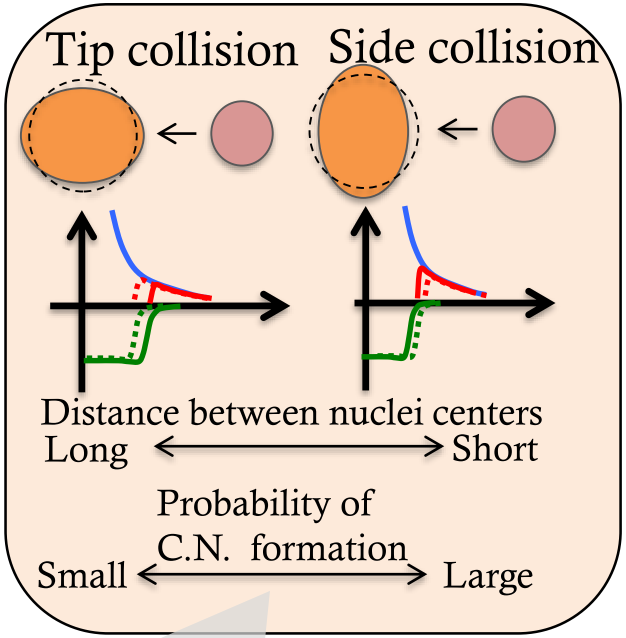

This was discussed
at lanthanoid target region.

D.J. Hinde *et al.*, Phys. Rev. Lett. **74**, 1295 (1995).
K. Nishio *et al.*, Phys. Rev. C **62**, 014602 (2000).

This was discussed
by theoretical calculations.

V. Zagrebaev *et al.*, Phys. Rev. C **78,** 034610 (2008).

σ_{ER} values are enhanced at the energy which corresponds to a compact collision geometry with the projectile impacting the side of the deformed target nucleus.

Summary

✓ Measurement of the barrier distribution
for the reactions ^{22}Ne+^{248}Cm, ^{26}Mg+^{248}Cm, ^{48}Ca+^{238}U and ^{48}Ca+^{248}Cm

✓ Fusion barrier B_{fu} (L ~ 0) directly derived.

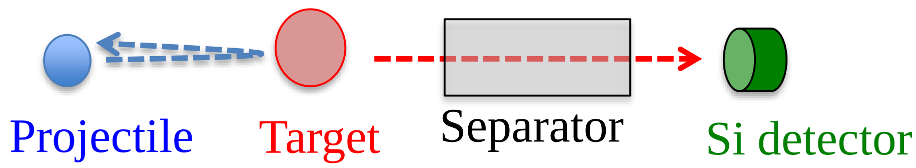

✓ Comparison with the experimental results and coupled-channels calculation

→ Barrier distributions are strongly affected by the deformation.

+ Improvement by excited states and 1n transfer

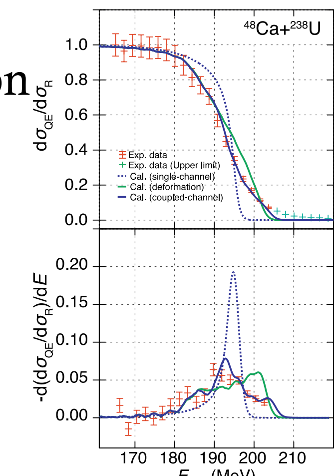

✓ Comparison with the experimental barrier distributions and σ_{ER}

→ Peaks of σ_{ER} appear between B_0 and B_{side}

→ σ_{ER} values are enhanced at the energy which corresponds to a compact collision

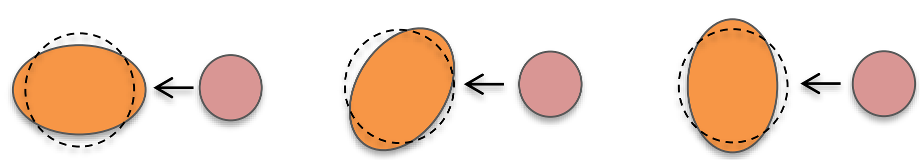

Thank you for your attention.